Effective Drusen Segmentation from Fundus Images for Age-related Macular Degeneration Screening

Huiying Liu, Yanwu Xu, Damon W.K. Wong, and Jiang Liu

Institute for Infocomm Research, A*STAR, Singapore

Abstract. Automatic screening of Age-related Macular Degeneration (AMD) is important for both patients and ophthalmologists. The major sign of contracting AMD at the early stage is the appearance of drusen, which are the accumulation of extracellular material and appear as yellow-white spots on the retina. In this paper, we propose an effective approach for drusen segmentation towards AMD screening. The major novelty of the proposed approach is that it employs an effective way to train a drusen classifier from a weakly labeled dataset, meaning only the existence of drusen is known but not the exact locations or boundaries. We achieve this by employing Multiple Instance Learning (MIL). Moreover, our proposed approach also tracks the drusen boundaries by using Growcut, with the output of MIL as initial seeds. Experiments on 350 fundus images with 96 of them with AMD demonstrates that our approach outperforms the state-of-the-art methods on the task of early AMD detection and achieves satisfying performance on the task of drusen segmentation.

1 Introduction

Age-related Macular Degeneration (AMD), after cataract and glaucoma, is the third leading cause of blindness worldwide and the first leading cause in the elderly [1] [2]. It is a kind of maculopothy that usually affects older adults and results in a loss of vision in the center of the visual field. Approximately 10% of patients 66 to 74 years of age will have findings of macular degeneration. The prevalence increases to 30% in patients 75 to 85 years of age. According to the statistical data of World Health Organization, till 2010, there were nearly 2 million occurrences of AMD in the United States. The number is projected to be over 5 million in 2050 (http://www.who.int/research/en/).

Population based AMD screening is in necessity for its increasing prevalence. However, symptoms (e.g., vision scotoma and distortion) at the early stage of AMD are generally not obvious to be observed. So it is usually late when patients are found out to have contracted AMD. As a result of that, the vision of those patients may be permanently lost. Therefore, it is of great importance to detect AMD at the early stage, and patients can thus take treatment to prevent it from getting worse. For the patients already diagnosed with AMD, accurate grading

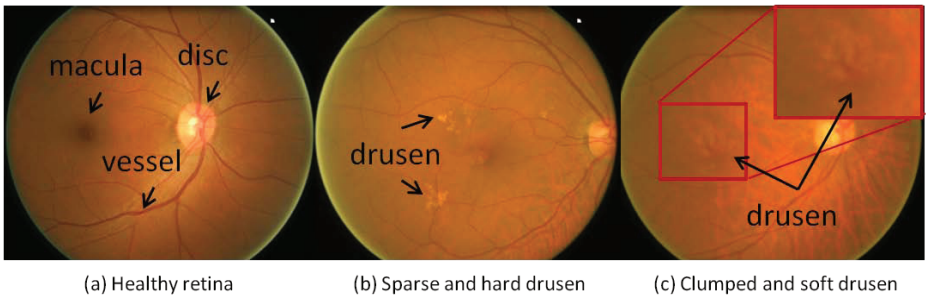

Fig. 1. Examples of fundus images with and without drusen. (a) A healthy fundus image. (b) A fundus image with sparse drusen. (c) A fundus image with clumped drusen, of poor image quality.

is important to customize a suitable treating strategy. Regular screening is a potential way to detect early AMD and grade AMD. However, manual detection and grading of AMD are time consuming and labor intensive. More importantly, because the grading is usually subjective (graded by human clinicians), a certain degree of inaccuracy may be introduced.

Automatic AMD screening brings profits for both patients and ophthalmologists, hence it has attracted much research effort in these years. The major sign of early AMD is the appearance of drusen [3][4]. Drusen appear as yellow-white spot on digital fundus image, which is the mainstream and most popular imaging modality for AMD diagnosis. Examples of drusen are shown in Figure 1 (b) and (c). Drusen detection has significant importance for early AMD detection, while drusen segmentation is important for AMD grading. Here we refer to drusen detection as identifying the existence of drusen in a fundus image, while drusen segmentation as finding the location and boundary of drusen.

In this paper, we propose a novel method which is not only able to detect early AMD but also segment drusen at the same time. The flowchart of the proposed method is shown in Figure 2. Our method first extracts local extreme points, i.e., maximum points and minimum points, in scale space. The maximum points are considered as potential drusen candidates. Edge Direction Histogram (EDH), SPIN feature, Gabor coefficients, intensity, position, and contrast are extracted at these maximum points. Then Multiple Instance Learning (MIL) is used to train a classifier from the weakly labeled data to classify each maximum points as drusen or non-drusen [5]. For a fundus image, if drusen are detected, it will be classified as early AMD. Finally, if drusen are detected, Growcut is employed to segment drusen [6]. The maximum points classified as drusen are used as foreground seeds. The ones classified as non-drusen, together with the minimum points, are used as background seeds. These seeds are fed into Growcut to get boundaries of drusen.

The contribution of this paper is that we propose an effective approach of drusen segmentation for AMD screening. The major contributions of this ap-

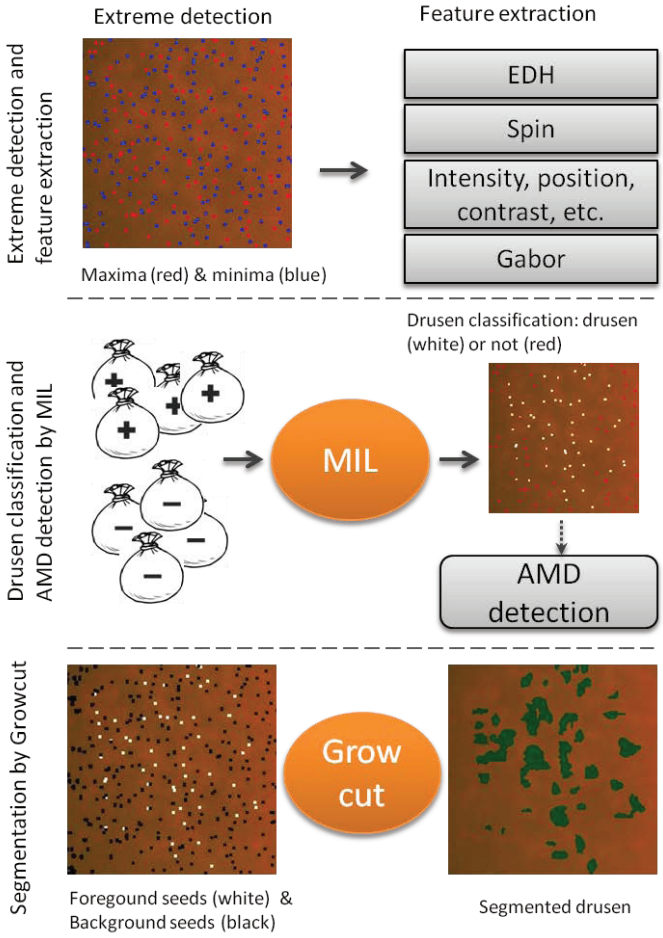

Fig. 2. The flowchart of the proposed method.

proach are as follows. 1) It is not only able to detect AMD but also to track the locations and boundaries of drusen for further AMD grading. 2) It employs Multiple Instance Learning (MIL) to train the detectors from a weakly labeled dataset thus significantly reduces the need for manual labeling. 3) It employs Growcut to track the boundaries of drusen, by using the output of MIL as initial seeds.

In the rest of this paper, we will review the state-of-the-art methods in Section 2. Then we will detail in Section 3 the proposed drusen segmentation approach, including extreme points detection, feature descriptors, classification using MIL, and segmentation using Growcut. In Section 4, we will show the experimental results on both AMD detection and drusen segmentation. Finally, we will conclude this paper with future work in Section 5.

2 Related work

For the importance of automatic AMD screening, in recent years, lots of methods have been proposed for drusen segmentation and AMD detection. The existing drusen segmentation methods can be classified into three major categories. The first category, consisting of the earliest drusen segmentation methods, is based on local maxima, e.g., the geodesic method [7]. These methods first detect local maxima, then further classify the candidates according to contrast, size and shape. The second category consists of the local threshold based methods, e.g., Histogram based Adaptive Local Thresholding (HALT) [8], and Otsu method based adaptive threshold [9]. The third category includes the ones from frequency domain, e.g., wavelet [10], Fourier transform [11], and amplitude-modulation frequency modulation (AM-FM) [12].

There are some other methods, e.g., background modeling method [13] and saliency based method [11]. The background modeling method first segments the healthy structure of eye and blood vessels. The inverse of the healthy parts provide the drusen detection result. The saliency based method first detects the salient regions then classifies them as blood vessel, hard exudates or drusen. In [14], a general framework is proposed to detect and characterize target lesions almost instantaneously. Within the framework, a feature space, including the confounders of both true positive (e.g., dursen near to other drusen) and false positive samples (e.g., blood vessels), is automatically derived from a set of reference image samples. Then Haar filter is used to build the transformation space and PCA is used to generate the optimal filter.

The performance of drusen segmentation based AMD detection methods is restricted by the accuracy of drusen segmentation. To bypass drusen segmentation, in recent years, researchers have started to seek for methods detecting AMD directly from fundus images, without drusen segmentation. These methods describe an image with locally extracted features, where the features are fed into a classifier to decide whether the image contains drusen or not. An early attempt in this direction was a histogram based representation followed by Case-Based Reasoning [15]. Good results were produced, however observations indicated that relying on the retinal image colour distribution alone was not sufficient. Thus, the authors further proposed a method by using a spatial histogram technique to include colour and spatial information [16]. The latest work from the same team comprises a hierarchical image decomposition mechanism, founded on either a circular and angular partitioning or a pyramid partitioning. The resulting decomposition is then stored in a tree structure to which a weighted frequent subtree mining algorithm is applied. The identified sub-graphs are then incorporated into a feature vector representation (one vector per image) to which classification techniques can be applied [17][18]. The latest methods in this category include Biologically Inspired Feature (BIF) based method [19] and Hierarchical Word Image representation and SPIN features based method named Thalia [20].

Although the methods detecting AMD without drusen segmentation show some progress, drusen segmentation has its importance in AMD grading. The severity of AMD is usually measured according to position, size, type (hard or

soft), together with geographic atrophy and other symptoms. The overlap of drusen with macula is used to measure the severity of AMD [21] [22].

3 The proposed method

As shown in Figure 1, drusen appear as yellow-white spots on fundus images. The visual properties that discriminate drusen from the other structures of retina are summarized as follows, together with the corresponding strategy adopted to describe the property.

1. Drusen appear brighter than the healthy part, except the optical disk, of the retina (Figure 1). However, the light on the fundus image is not uniform thus drusen are not globally brighter. We detect local maximum points as drusen candidates and use contrast as a feature for classification.
2. Drusen don't have exact size thus we extract local maxima at multiple scales to detect drusen of different sizes.
3. Drusen are near round spots. Shape distinguishes drusen from the regions near vessels which are likely to be detected as drusen but drusen don't have rigid shape (Figure 1 (b) and (c)). We adopt edge direction histogram to describe shape and adopt SPIN feature to describe the color-spatial structure of drusen.
4. Drusen may appear differently due to different imaging conditions (Figure 1 (c)). Thus we adopt local texture, which is more robust to lighting condition than color. Gabor coefficients are used for this purpose.

The above detected and described maximum points are fed into multiple instance learning to train a classifier, which is used for drusen classification.

Tracking drusen boundaries is facing two difficulties. First, drusen have two types, hard drusen and soft drusen. Soft drusen usually don't have sharp boundary thus result in the difficulty to obtain the boundary. Second, in severe condition, drusen may clump together thus increase the difficulty of drusen segmentation. Figure 1 (c) shows an example of soft and clumped drusen. To address these difficulties, we employ Growcut, with the detected drusen position as seeds, to track drusen boundaries.

The flowchart of the proposed approach is shown in Figure 2. The details of the methods are stated in the rest of this section.

3.1 Extremum points detection

Like SIFT[23], we detect local extrema in the scale space. We first construct the Gaussian space of the image. At each level, the image is convolved with a Gaussian function,

$$L(i, j, \sigma_k) = G(i, j, \sigma_k) * I(i, j), \tag{1}$$

where I is the input image, (i, j) is the position in the image, $G(i, j, \sigma_k)$ is a Gaussian function with standard variance of σ_k, and $*$ is the convolution

operator. Then from the Gaussian space,we construct the Laplacian space as follow,

$$\begin{aligned} D(i,j,\sigma_k) &= (G(i,j,\sigma_k) - G(i,j,\sigma_{k+1})) * I(i,j) \\ &= L(i,j,\sigma_k) - L(i,j,\sigma_{k+1}), \end{aligned} \tag{2}$$

The Laplacian space has one less level than the Gaussian Space. We adopt $\sigma = \sqrt{2}^{\{-1,0,1,\ldots,12\}}$. A pixel is determined to be a maximum if it is a local maximum in the Laplacian space. The local window used to determine the maximum is $3 \times 3 \times 3$. Thus, we detect maximum points at scales $\sigma = \sqrt{2}^{\{0,1,\ldots,10\}}$.

In Equation (2), $D(i,j,\sigma) = 0$ when $i^2 + j^2 = \frac{2a^2\sigma^2 \log(a^2)}{a^2-1}$. Here $a = \frac{\sigma_{k+1}}{\sigma_k}$. When $a = \sqrt{2}$, the radius of detected drusen at scale σ is $r = 1.67\sigma$. Thus the minimal and maximal diameters of detected drusen are 3 and 108 pixels respectively. Figure 2 (the top left block) illustrates an example of detected extreme points.

3.2 Feature description

The characteristics distinguishing drusen from the background are intensity, shape, size, contrast and texture. Further, drusen usually distribute around macula. The following features are adopted to describe these characteristics.

Edge Direction Histogram is used to describe the shape of the local maxima at the corresponding scale. The histogram is weighted by the gradient magnitude and the Gaussian function. The edge direction histogram of a maximum point is

$$H(i,j,o,\sigma) = \sum_{(i',j') \in I, O(i',j',\sigma)=o} M(i',j',\sigma) \times G(i',j',\sigma) \tag{3}$$

where $O(i,j,\sigma)$ and $M(i,j,\sigma)$ are respectively the orientation and magnitude of gradient at position (i,j) and scale σ. In our experiment, the number of bins of the histogram is set as 8.

Intensity. Drusen are bright spots on the fundus thus intensity is an useful visual descriptor of drusen. We adopt intensity at the Gaussian space at corresponding scale instead of the original image for better robustness.

Contrast. Drusen are locally brighter than neighbors thus contrast is an important indicator of drusen. The value of each maximum at the Laplacian space is used as contrast.

Size. The size of drusen is in general different compared to the optic disc and vessels. In our method, the scales of the maxima are used to indicate size.

Hessian. In SIFT, the ratio of the maximum and minimum eigen values of the Hessian matrix is used to discriminate edge and spot. We adopt this value to distinguish blood vessels and drusen.

Distance to macula. Drusen usually appear near the macula. Furthermore, the drusen nearer to the macula are more clinically important than the ones farther away. Therefore, spatial distance to macula is used as a feature for drusen classification.

Gabor coefficients. Gabor coefficients at 5 scales and 8 orientations are used as features to describe the local texture.

SPIN feature. Drusen typically appear as circular, roundish spots in the retina. To make use of this characteristic, SPIN features is used to embed local neighborhood context [24]. The SPIN feature encodes the distribution of image brightness values in the neighborhood of a particular reference (center) point. This is achieved by a soft-assigned histogram of the intensity values of pixels located at a distance d from the pixel (i, j). That is,

$$f_{(i,j)}(d, v) = \sum_{(i',j') \in \Gamma(i,j)} \exp\left(-\frac{(\|(i', j') - (i, j)\| - d)^2}{2\alpha^2} - \frac{\|I(i', j') - v\|^2}{2\beta^2} \right) \quad (4)$$

here $\|.\|$ means Euclid distance. $\Gamma(i, j)$ is the neighborhood of (i, j). v is the gray value of the pixels. α and β are the parameters representing the soft width of the bins. In our implementation, the number of color bins is 8. The number of location bins and the scales are consistent with he ones used for extrema detection.

3.3 Classification by MIL

After detecting the local maxima, we adopt multiple instance learning to train a drusen detector [5]. MIL is a good choice for weakly labeled data. For MIL, each bag of samples share a label. A bag is labelled as positive if at least one sample in it is positive, conversely it is labelled as negative if all the samples in it are negative. It has been used in object detection and image categorization with good performance [25]. For drusen detection, labelling the presence of drusen is much easier than marking the boundary of drusen. Therefore, we employ multiple instance learning to train a drusen classifier from the weakly labeled data. The mi-SVM algorithm [26] is used in our work. This algorithm formulates multiple instance learning as a maximum margin problem which can be solved by an extension of the generalized Support Vector Machines (SVM).

In mi-SVM, each instance label is subjected to constraints defined by the (positive) bag labels. This is to ensure label consistency with the bag label. The goal is then to maximize the soft-margin jointly over hidden label variables and a kernelized discriminant function. The mixed integer objective function formulation of mi-SVM as a generalized soft-margin SVM in its primal form is defined as:

$$\min_{\{y_i\}} \min_{\mathbf{w},b,\xi} \frac{1}{2}\|\mathbf{w}\|^2 + C\sum_i \xi_i,$$

$$s.t. \begin{cases} \forall i: & y_i(\langle \mathbf{w}, x_i \rangle + b) \geq 1 - \xi_i, \\ & \xi_i \geq 0, \\ & y_i \in \{-1, 1\}, \\ \forall I: & \sum_{i \in I} \frac{y_i+1}{2} \geq 1, \ \textit{if } Y^I = 1 \\ & y_i = -1|_{i \in I}, \ \textit{if } Y^I = -1. \end{cases} \quad (5)$$

where $\mathbf{w} \in \mathbb{R}^d, b \in \mathbb{R}, \xi$ are the weight vector, offset and slack variables of SVM.

As y_i is a discrete variable, solving the mi-SVM problem to find the optimal labels and hyperplane, is a combinatorial mixed integer programming problem. The heuristic quadratic programming (QP) scheme proposed by [26] to optimize this objective function begins by initializing all instance labels from the positive labeled bags to be 1 and alternates between optimizing the parameters w and b for the SVM solution with the current imputed labels, and assigning y based on the resulting classification boundary. After each step, the constraints in Equation 5 are checked and re-enforced.

3.4 Segmentation by Growcut

After classification, we obtain the locations of drusen, without boundary. We employ Growcut to track the drusen boundary. While local threshold and region grow methods are employed in other works, we found that local threshold method fails in the situation of clumped drusen and region grow has the problem of leaking. Growcut is able to track the boundary with small number of seeds [6]. It was verified to be effective in medical image segmentation.

Growcut is a celluar automata based image segmentation method. A cellular automaton is a triplet $A = (S, N, \delta)$, where S is an non-empty state set, N is the neighbor hood system, and $\delta : S^N \to S$ is the local transition function (rule). This function defines the rule of calculating the cell's state at $t + 1$ time step, given the states of the neighborhood cells at previous time step t. The cell state S_p in our case is actually a triplet $(l_p, \theta_p, \overrightarrow{C}_p)$ - the label l_p of the current cell, 'strength' of the current cell $\theta_p \in [0, 1]$, and cell feature vector $\overrightarrow{C}_p$, defined by the image (the RGB color vector). Growcut is an iterative method. At each step, the seeds attack their neighbors until all the pixels are labeled.

Growcut was designed as an interactive foreground segmentation algorithm, with users manually mark several foreground seeds and background seeds. In [27], unsupervised Growcut, with random seeds and labels, is used for medical image segmentation. We apply it in a supervised mode, with the seeds and labels determined in the classification process.

While detecting the extremum points, the minimum points are almost all non-drusen. Among the maximum points, some (most) of them are non-drusen and classified correctly as non-drusen. These points are then used as background seeds. and the points classified as drusen are used as foreground seeds. These seeds are fed into Growcut to track the boundary of drusen [6]. An example of Growcut seeds and segmentation result can be found in Figure 2.

While labeling, we found that if the whole image is labelled at one time, Growcut is not able to give satisfying result. Therefore, for each drusen seed, we perform Growcut on the local rectangle patch, which is the minimum bounding box covering the drusen seeds and at least 5 non-drusen seeds.

4 Experiments

The experiments are performed on ACHIKO-D350 [28], which is, as far as we know, the only dataset with drusen boundaries marked. It consists of 350 population-based images from the Singapore Eye Malay Study, consisting of 96 clinically verified drusen images and 254 non-drusen images. Each image has a resolution of 3072x2048 and had been acquired using a 45 FOV Canon CR-DGi retinal fundus camera with a 10D SLR backing. Among the 96 images, 45 ones of left eyes and 51 ones of right eyes. The boundary of drusen are semi-manually marked out. Besides drusen boundaries, the position of the macula is also manually marked. In experiments, the images are resized to 1024*683.

The measurements adopted in experiments include sensitivity, specificity, average precision (the average of sensitivity and specificity), and the Area Under Curve (AUC) of the Receiver Operating Characteristic (ROC). Sensitivity (true positive rate) and specificity (true negative rate) are defined in Eq. 6.

$$\begin{aligned} Sensitivity &= \frac{True\,positives}{Positives}, \\ specificity &= \frac{True\,negatives}{Negatives}. \end{aligned} \tag{6}$$

Receiver operating characteristic is the true positive rate (sensitivity) vs. false positive rate (1-specificity) curve.

4.1 Computing time

In our method, the drusen classifier using MIL is trained off-line. After training the classifier, our workflow consists of four main steps: i) extreme point detection; ii) feature description; iii) multiple instance learning; and iv) drusen segmentation using growcut. We recorded the computational time of each step for processing one image of 1024*768 as follows: 14s, 7s, 1.5s, and 10s for i), ii), iii) and iv), respectively. So, the total time for one image is 32.5 seconds. Note that our method is implemented with unoptimized MATLAB code on a workstation with 2.4GHz dual CPU and 64GB memory. The time cost can be largely reduced by optimizing the code and using an upgraded server, which easily make our method acceptable for clinical application.

4.2 Feature selection

The features used in our work are of four types, Edge Direction Histogram (EDH), Macula Related Feature (MRF, consists of distance to macula, scale, intensity, contrast, and Hessian value), Gabor, and SPIN. The performances of the single features are shown in Table 1. From the result, we can see that 1) EDH and macula related feature are able to provide higher sensitivity with lower specificity and 2) in means of average precision, macula related feature gives the best performance.

Table 1. Performance of single features

Feature	Sensitivity	Specificity	Avg precision
EDH	80.44	55.61	68.03
MRF	90.06	75.79	82.93
Gabor	76.75	82.7	79.72
SPIN	82.67	78.86	80.76

The combination of all four types of features is used in our paper, because it gives better performance than any other forms of combinations, as shown in Table 2. We can see that the result is consistent with the one in Table 1.

Table 2. Performance of feature combinations

Feature combination	Sensitivity	Specificity	Avg precision
MRF+EDH+Gabor+SPIN	90.62	86.86	88.74
- MRF	84.84	85.17	85
- EDH	90.59	86.87	88.73
- Gabor	90.92	83.24	87.08
- SPIN	88.43	86.03	87.23

Summing up the results in Table 1 and Table 2, we can draw the conclusion that the macula related feature performs the best. It is able to provide high sensitivity but relatively lower specificity. Other features combined are able to keep the high sensitivity while increase the specificity.

4.3 Results on AMD detection

To test the performance of AMD detection, we compare our method with the BIF [19] based method and the Thalia system [20]. The results of these two methods, on the same dataset, are reported in their papers. To make the comparison fair and objectively, in experiment, we adopt the same setting with the two methods, meaning randomly choose 50 positive sample and negative samples as training data and the left ones as test data. The experiments are run 10 times. The means and standard deviations of sensitivity, specificity, the average precision, and AUC are shown in Table 3. From the table, we can see that our method outperforms the two methods on the task of AMD detection. It is worth to point out that our approach achieves the high sensitivity of 100%, with the high specificity of 96.76. The standard deviation of our method is also the lowest.

Table 3. Performance comparison on early AMD detection

	sensitivity	specificity	Average precision	AUC
BIF[19]	86.3± 3.2	91.9 ± 3.1	89.11±1.35	NA
Thalia[20]	NA*	NA	95.46±0.94	NA
Proposed	100±0	96.76±1.16	98.38±0.58	97.26±0.98

*NA means Not Available.

Figure 3 shows the top 10 images that are most likely to have AMD and the 10 images that are least likely to have AMD. All the 20 images are correctly classified. From the result, we can see that the approach is robust to image condition.

4.4 Results of drusen segmentation

Then we further evaluate the performance of drusen segmentation, by means of sensitivity, specificity, and average precision. Since drusen classification, meaning classifying the maximum points as drusen or not, is the basis of drusen segmentation, we also show the results of drusen classification.

As our method is weakly supervised, we compare it with the corresponding fully supervised method, meaning support vector machine using the manual label as training data. The comparison result is shown in Table 4. Figure 4 and 5 show the drusen segmentation result of the SVM based method and the MIL based method. Refer to Table 4, Figure 4 and Figure 5, we find that the weakly supervised MIL gives lower sensitivity but higher specificity compared to the fully supervised learning SVM.

Table 4. The performance of the proposed method

	classification			segmentation		
	sensitivity	specificity	average precision	sensitivity	specificity	average precision
SVM	90.23±0.60	87.08±0.28	88.66±0.32	67.77±0.51	94.36±0.12	81.07±0.24
MIL	50.59±6.93	90.89±3.37	70.74±2.11	40.54±6.26	96.17±1.44	67.85±2.48

5 Conclusion

In this paper, we propose an effective AMD screening approach. This approach employs multiple instance learning to reduce the need for manual labelling train-

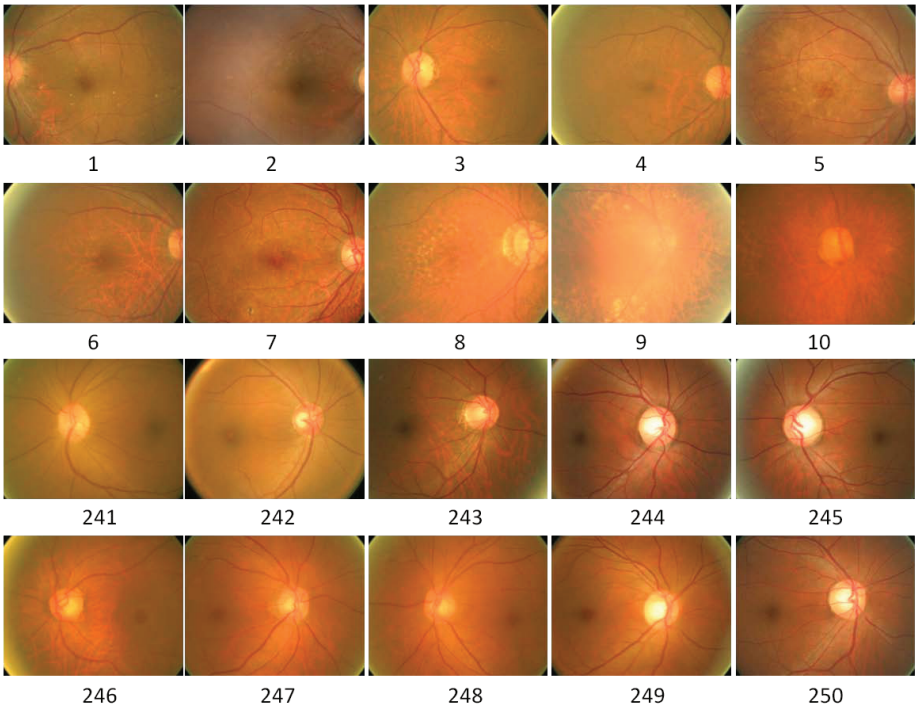

Fig. 3. Examples of AMD detection. The top two rows: the 10 images that are most likely to have AMD. The bottom two rows: the 10 images that are least likely to have AMD. The number below each image is the ranking number in the classification result.

ing data. As shown by the experimental results, on the task of AMD detection, the proposed approach outperforms the state-of-the-art methods. On the task of drusen segmentation, its performance is satisfying compared with the fully supervised result. One important application of drusen segmentation is AMD grading. In our future work, we will extend our approach to grade the severity of AMD.

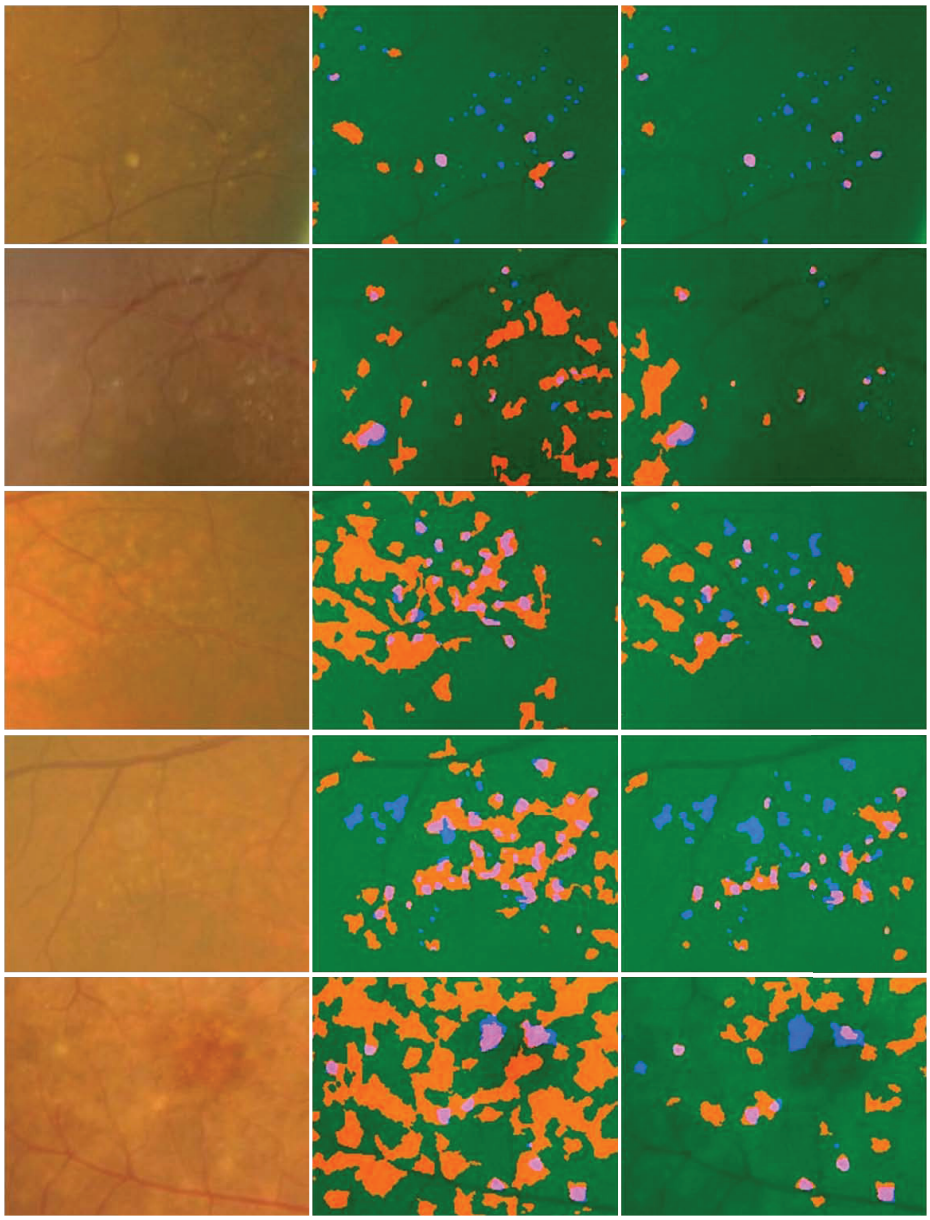

Fig. 4. Examples of drusen segmentation. The image are the 1-5th in Figure 3. The first column shows the drusen regions of the fundus images. The second and third columns show the drusen segmentation results of the SVM based method and the MIL based method. The green background is the green channel of the fundus image, the regions in blue are the false negative. The regions in purple are the true positive and the ones in orange are false positive.

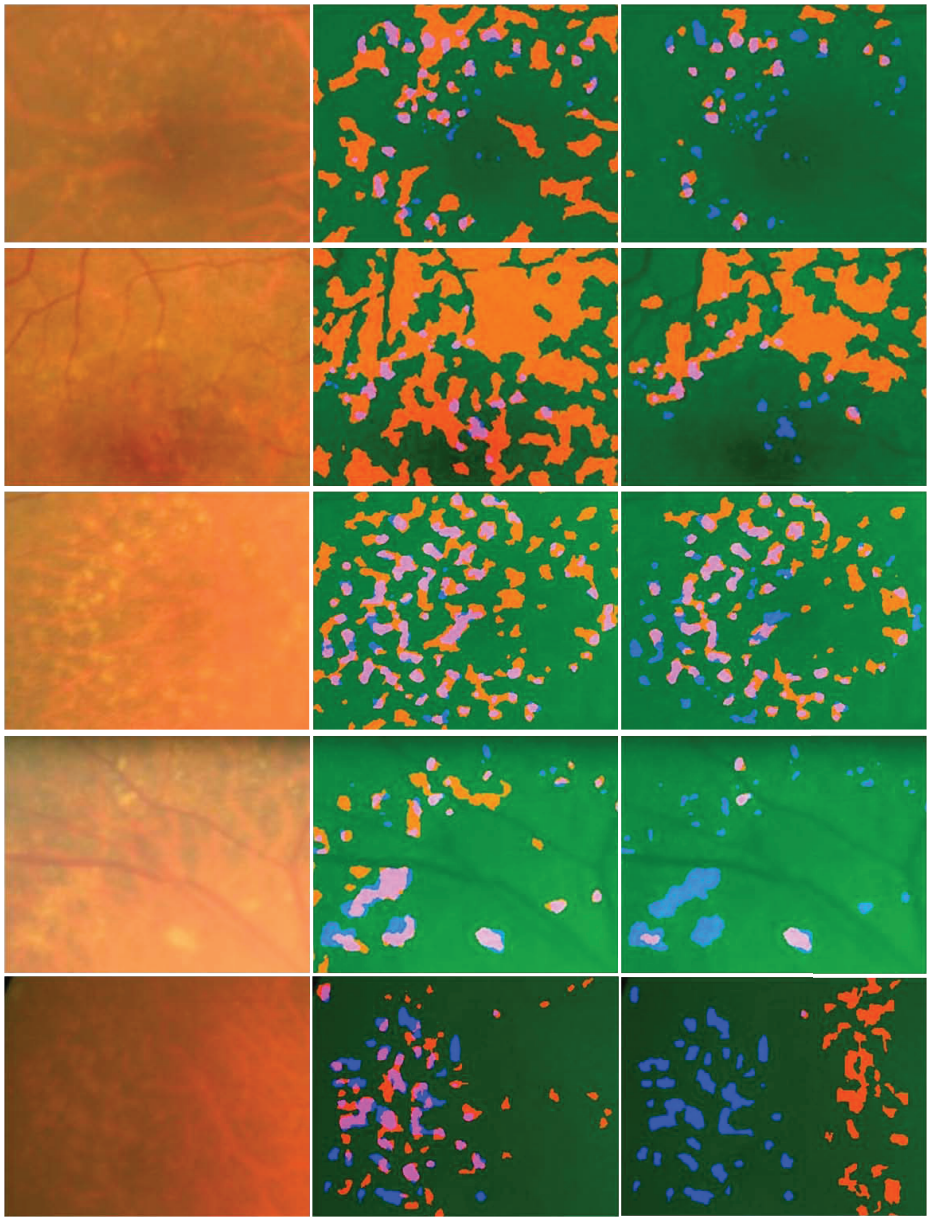

Fig. 5. Examples of drusen segmentation. The image are the 6-10th in Figure 3. The first column shows the drusen regions of the fundus images. The second and third columns show the drusen segmentation results of the SVM based method and the MIL based method. The green background is the green channel of the fundus image, the regions in blue are the false negative. The regions in purple are the true positive and the ones in orange are false positive.

References

1. Kawasaki, R., Yasuda, M., Song, S.J., Chen, S.J., Jonas, J.B., Wang, J.J., Mitchell, P., Wong, T.Y.: The prevalence of age-related macular degeneration in asians: a systematic review and meta-analysis. Ophthalmology **117** (2010) 921–927
2. Jager, R.D., Mieler, W.F., Miller, J.W.: Age-related macular degeneration. New England Journal of Medicine **358** (2008) 2606–2617
3. Bressler, N.M., Bressler, S.B., Fine, S.L.: Age-related macular degeneration. Survey of ophthalmology **32** (1988) 375–413
4. De Jong, P.T.: Age-related macular degeneration. New England Journal of Medicine **355** (2006) 1474–1485
5. Dietterich, T.G., Lathrop, R.H., Lozano-Pérez, T.: Solving the multiple instance problem with axis-parallel rectangles. Artificial intelligence **89** (1997) 31–71
6. Vezhnevets, V., Konouchine, V.: Growcut: Interactive multi-label nd image segmentation by cellular automata. In: Proc. of Graphicon. (2005) 150–156
7. Ben Sbeh, Z., Cohen, L.D., Mimoun, G., Coscas, G.: A new approach of geodesic reconstruction for drusen segmentation in eye fundus images. IEEE Transactions on Medical Imaging **20** (2001) 1321–1333
8. Rapantzikos, K., Zervakis, M., Balas, K.: Detection and segmentation of drusen deposits on human retina: Potential in the diagnosis of age-related macular degeneration. Medical image analysis **7** (2003) 95–108
9. Smith, R.T., Chan, J.K., Nagasaki, T., Ahmad, U.F., Barbazetto, I., Sparrow, J., Figueroa, M., Merriam, J.: Automated detection of macular drusen using geometric background leveling and threshold selection. Archives of ophthalmology **123** (2005) 200
10. Brandon, L., Hoover, A.: Drusen detection in a retinal image using multi-level analysis. In: Medical Image Computing and Computer-Assisted Intervention-MICCAI. (2003) 618–625
11. Ujjwal, K., Chakravarty, A., Sivaswamy, J.: Visual saliency based bright lesion detection and discrimination in retinal images. In: IEEE 10th International Symposium on Biomedical Imaging: From Nano to Macro. (2013) 1428–1431
12. Barriga, E., Murray, V., Agurto, C., Pattichis, M., Russell, S., Abramoff, M., Davis, H., Soliz, P.: Multi-scale am-fm for lesion phenotyping on age-related macular degeneration. In: IEEE International Symposium on Computer-Based Medical Systems. (2009) 1–5
13. Köse, C., Sevik, U., Gencalioglu, O., Ikibas, C., Kayikicioglu, T.: A statistical segmentation method for measuring age-related macular degeneration in retinal fundus images. Journal of medical systems **34** (2010) 1–13
14. Quellec, G., Russell, S.R., Abràmoff, M.D.: Optimal filter framework for automated, instantaneous detection of lesions in retinal images. IEEE Transactions on Medical Imaging **30** (2011) 523–533
15. Hijazi, M.H.A., Coenen, F., Zheng, Y.: Retinal image classification using a histogram based approach. (In: IEEE International Joint Conference on Neural Networks) 3501–3507
16. Hijazi, M.H.A., Coenen, F., Zheng, Y.: Retinal image classification for the screening of age-related macular degeneration. In: Research and Development in Intelligent Systems XXVII. (2011) 325–338
17. Hijazi, M.H.A., Jiang, C., Coenen, F., Zheng, Y.: Image classification for age-related macular degeneration screening using hierarchical image decompositions and graph mining. In: Machine Learning and Knowledge Discovery in Databases. (2011) 65–80

18. Zheng, Y., Hijazi, M.H.A., Coenen, F.: Automated "disease/no disease" grading of age-related macular degeneration by an image mining approach. Investigative ophthalmology & visual science **53** (2012) 8310–8318
19. Cheng, J., Wong, D.W.K., Cheng, X., Liu, J., Tan, N.M., Bhargava, M., Cheung, C.M.G., Wong, T.Y.: Early age-related macular degeneration detection by focal biologically inspired feature. In: IEEE International Conference on Image Processing. (2012) 2805–2808
20. Wong, D.W., Liu, J., Cheng, X., Zhang, J., Yin, F., Bhargava, M., Cheung, G.C., Wong, T.Y.: Thalia-an automatic hierarchical analysis system to detect drusen lesion images for amd assessment. In: IEEE International Symposium on Biomedical Imaging. (2013) 884–887
21. Medhi, J.P., Nath, M.K., Dandapat, S.: Automatic grading of macular degeneration from color fundus images. In: World Congress on Information and Communication Technologies. (2012) 511–514
22. Liang, Z., Wong, D.W., Liu, J., Chan, K.L., Wong, T.Y.: Towards automatic detection of age-related macular degeneration in retinal fundus images. In: IEEE International Conference on Engineering in Medicine and Biology Society. (2010)
23. Lowe, D.: Distinctive image features from scale-invariant keypoints. International Journal of Computer Vision **60** (2004) 91–110
24. Johnson, A.E., Hebert, M.: Using spin images for efficient object recognition in cluttered 3d scenes. IEEE Transactions on Pattern Analysis and Machine Intelligence **21** (1999) 433–449
25. Qi, G.J., Hua, X.S., Rui, Y., Mei, T., Tang, J., Zhang, H.J.: Concurrent multiple instance learning for image categorization. In: IEEE Conference on Computer Vision and Pattern Recognition. (2007) 1–8
26. Andrews, S., Tsochantaridis, I., Hofmann, T.: Support vector machines for multiple instance learning. In: Advances in Neural Information Processing Systems (NIPS). (2003)
27. Ghosh, P., Antani, S.K., Long, L.R., Thoma, G.R.: Unsupervised grow-cut: cellular automata-based medical image segmentation. In: IEEE International Conference on Healthcare Informatics, Imaging and Systems Biology (HISB). (2011) 40–47
28. Liu, H., Xu, Y., Wong, D.W.K., Laude, A., Lim, T.H., Liu, J.: Achiko-d350: A dataset for early amd detection and drusen segmentation. In: Ophthalmic Medical Image Analysis (MICCAI workshop). (2014)